

Journal of Cybernetics and Informatics

published by

**Slovak Society for
Cybernetics and Informatics**

Volume 7, 2008

<http://www.sski.sk/casopis/index.php> (home page)

ISSN: 1336-4774

A SLIDING MODE POSITION CONTROL OF A SYNCHRONOUS MACHINE USING NEURAL NETWORK DISTURBANCE OBSERVER

Abdel Ghani Aissaoui*, **Mohamed Abid***, **Hamza Abid****, **Ahmed Tahour*****, **Abdel
kader Zeblah***

***) IRECOM Laboratory, University of Sidi Bel Abbes, 22000, Algeria,**

*****) AML Laboratory, University of Sidi Bel Abbes, 22000, Algeria**

*****) University of Bechar, 08000, Algeria**

Corresponding author e-mail: IRECOM_aissaoui@yahoo.fr

Abstract: In this paper, we propose a sliding mode technique to control the field-oriented synchronous machine. The sliding mode controller is designed for a class of non linear dynamic systems to tackle the problems with model uncertainties, parameter fluctuations and external disturbances. Our aim is to make the position control robust to parameter variations. The use of the nonlinear sliding mode method provides very good performance for motor operation and robustness of the control law despite the external/internal perturbations. An observer is considered to overcome the problem of torque disturbance. A load torque observer is designed based on neural network technique without affecting the overall system response. Simulation results are given to highlight the performance of the proposed control technique under load disturbances and parameter uncertainties.

Keywords: synchronous machine, sliding mode control, Neural load torque observer, position control.

1 INTRODUCTION

Since the work of V. I. Utkin proposed in 1977 [1], significant interest on variable structure systems (VSS) has been generated in the control research community worldwide. The variable structure control (VSC) possesses high robustness using the sliding mode control that can offer many good properties such as good performance against unmodelled dynamics, insensitivity to parameter variation, complete rejection of disturbances, and fast dynamic [2].

Sliding mode is originally conceived as system motion for dynamic whose essential open loop behavior can be modeled adequately with ordinary differential equations.

Variable structure control (VSC) with sliding mode or sliding mode control (SMC), is one of the effective non linear robust control approaches since it provides system dynamics with an invariance property to uncertainties once the system dynamics reach the sliding surface [1, 3, 4]. The main disadvantage of this approach is the high switching frequency of the control action or chattering that VSC system exhibit. Introducing a boundary layer (BL) is one of the most common techniques used, with the cost of an important degradation in tracking performance [5].

The new industrial applications necessitate speed/position variators having high dynamics performances, a good precision in permanent regime, and a high capacity of overload on all range of speed and a robustness to different perturbations. The variable structure control (VSC) possesses this robustness using the sliding mode control that can offer many good properties such as good performance against unmodeled dynamics, insensitivity to parameter variation, external disturbance rejection and fast dynamic. These advantages of sliding mode control can be employed in the position and speed control of a synchronous machine [1, 6-8].

In this paper the application of sliding mode control in synchronous position control is described. The organization of this paper is as follows: in section 2, the vector control principle for synchronous motor drive is presented; in section 3, the proposed controller is described, and used to control the position synchronous motor, and by the way, a neural load torque observer is developed based on neural network. Simulation results are given to show the effectiveness of this controller and finally conclusions are summarized in the last section.

2 SYNCHRONOUS MOTOR DYNAMIC MODEL

2.1. Machine equations

The more comprehensive dynamic performance of a synchronous machine can be studied by synchronously rotating d-q frame model known as Park equations. The dynamic model of synchronous motor in d-q frame can be represented by the following equations [9, 10]:

$$\begin{aligned} v_{ds} &= R_s i_{ds} + \frac{d}{dt} \phi_{ds} - \omega \phi_{qs} \\ v_{qs} &= R_s i_{qs} + \frac{d}{dt} \phi_{qs} + \omega \phi_{ds} \\ v_f &= R_f i_f + \frac{d}{dt} \phi_f \end{aligned} \quad (1)$$

The mechanical equation of synchronous motor can be represented as:

$$J \frac{d}{dt} \Omega = T_e - T_L - B\Omega \quad (2)$$

Where the electromagnetic torque is given in d-q frame:

$$T_e = p(\phi_{ds} i_{qs} - \phi_{qs} i_{ds}) \quad (3)$$

In which:

$$\Omega = \frac{d}{dt} \theta, \quad \theta = \int \Omega dt, \quad \omega = \frac{d}{dt} \theta_e = p \Omega, \quad \theta_e = p \theta.$$

The flux linkage equations are:

$$\begin{aligned} \phi_{ds} &= L_{ds} i_{ds} + M_{fd} i_f \\ \phi_{qs} &= L_{qs} i_{qs} \\ \phi_f &= L_f i_f + M_{fd} i_{ds} \end{aligned} \quad (4)$$

Where R_s – stator resistance, R_f – field resistance, L_{ds}, L_{qs} – respectively direct and quadrature stator inductances, L_f – field leakage inductance, M_{fd} – mutual inductance between inductor and armature, ϕ_{ds} and ϕ_{qs} – respectively direct and quadrature flux, ϕ_f –

field flux, T_e – electromagnetic torque, T_L – external load disturbance, p – pair number of poles, B – is the damping coefficient, J – is the moment of inertia, ω – electrical angular speed of motor. Ω – mechanical angular speed of motor, θ – mechanical rotor position, θ_e – electrical rotor position.

2.2. Description of the system

The schematic diagram of the position control system under study is shown in figure (1). The power circuit consists of a continuous voltage supply a three phase inverter whose output is connected to the stator of the synchronous machine [9]. The field current i_f of the synchronous machine, which determines the field flux level is controlled by voltage v_f . The parameters of the synchronous machine are given in the Appendix.

The self-control operation of the inverter-fed synchronous machine results in a rotor field oriented control of the torque and flux in the machine. The principle is to maintain the armature flux and the field flux in an orthogonal or decoupled axis. The flux in the machine is controlled independently by the field winding and the torque is affected by the fundamental component of armature current i_{qs} . In order to have an optimal functioning, the direct current i_{ds} is maintained equal to zero [10, 11].

Substituting (4) in (3), the electromagnetic torque can be rewritten for $i_f = \text{constant}$ and $i_{ds} = 0$ as follow:

$$T_e(t) = \lambda i_{qs}(t) \quad (5)$$

where $\lambda = pM_{fd}i_f$.

In the same conditions, it appears that the v_{ds} and v_{qs} equations are coupled. We have to introduce a decoupling system, by introducing the compensation terms emf_d and emf_q in which

$$\begin{aligned} emf_d &= \omega L_{qs} i_{qs}, \\ emf_q &= -\omega L_{ds} i_{ds} - \omega M_{af} i_f. \end{aligned} \quad (6)$$

Figure (1) shows the schematic diagram of the position control of synchronous motor using sliding mode control.

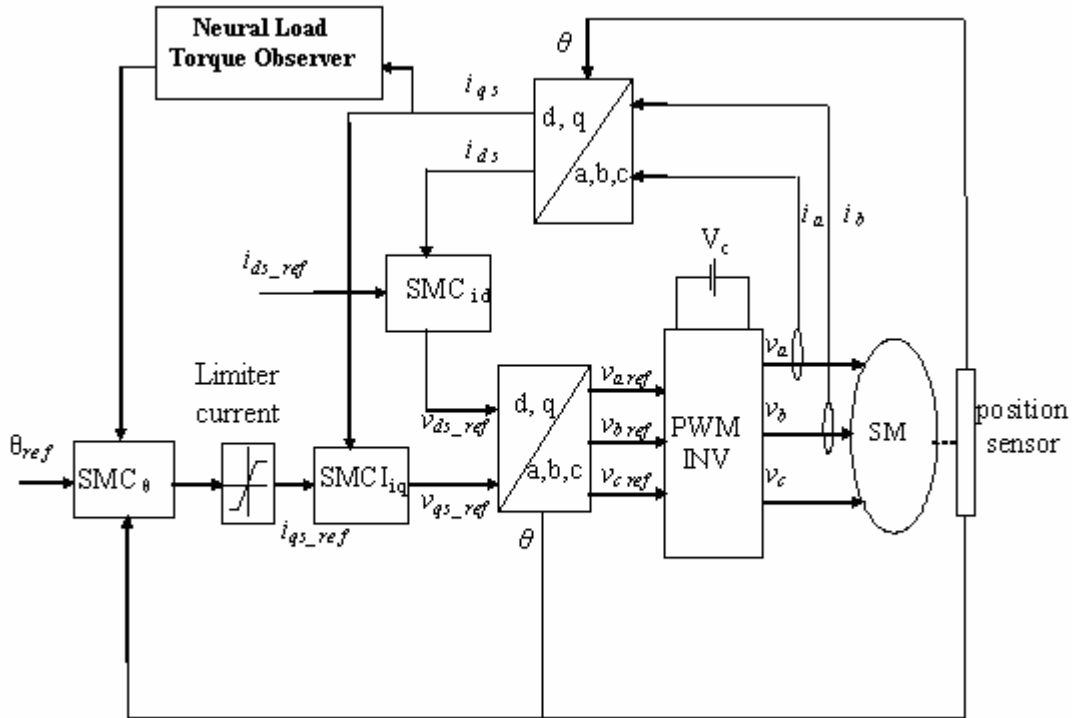


Figure 1. System Configuration of Field-Oriented Synchronous Motor.

The blocks SMC_{θ} , SMC_{ids} et SMC_{iqs} are regulators, the first is the sliding mode controller for position, the second is the sliding mode regulator for the direct current and the third is the sliding mode regulator for the quadrature current. The load torque is estimated by the “Neural load torque observer”. To avoid the appearance of an inadmissible value of current, a saturation bloc is used.

2.3. Voltage inverter

The power circuit of a three-phase bridge inverter using six switch device is shown in figure 2. The dc supply is normally obtained from a utility power supply through a bridge rectifier and LC filter to establish a stiff dc voltage source [12].

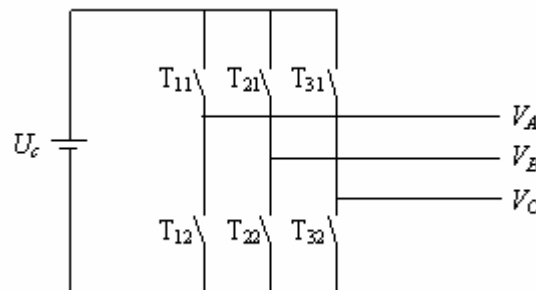


Figure 2. Voltage inverter

The switch T_{ci} ($c \in \{1, 2, 3\}$, $i \in \{1, 2\}$) is supposed perfect. The simple inverter voltage can be presented by logical function connection in matrix form as [12].

$$\begin{bmatrix} V_A \\ V_B \\ V_C \end{bmatrix} = \frac{1}{3} \begin{bmatrix} 2 & -1 & -1 \\ -1 & 2 & -1 \\ -1 & -1 & 2 \end{bmatrix} \begin{bmatrix} F_{11} \\ F_{21} \\ F_{31} \end{bmatrix} U_c, \quad (7)$$

where the logical function connection F_{c1} is defined as: $F_{c1} = 1$ if the switch T_{c1} is closed, $F_{c1} = 0$ if the switch T_{c1} is opened, U_c is the voltage feed inverter.

3 SLIDING MODE CONTROL

Consider a nonlinear system which can be represented by the following state space model in a canonical form [3, 13]:

$$\begin{aligned} \dot{x}^{(n)}(t) &= f(x(t), t) + g(x(t), t)u + d(t) \\ y(t) &= x(t) \end{aligned} \quad (8)$$

where $x = [x(t) \ \dot{x}(t) \dots x^{(n-1)}(t)]^T$ is the state vector, $f(x(t), t)$ and $g(x(t), t)$ are nonlinear functions, u is the control input, $d(t)$ is the external disturbances.

The objective of the control is to determine a control law $u(t)$ to force the system output $y(t)$ in (8) to follow a given bounded reference signal $y_d(t)$, that is, the tracking error $e(t) = y_d(t) - y(t)$ and its forward shifted values, defined as

$$\begin{aligned} e^{(i)}(t) &= y_d^{(i)}(t) - y^{(i)}(t) \\ &= x_d^{(i)}(t) - x^{(i)}(t), \quad (i = 1, \dots, n-1) \end{aligned} \quad (9)$$

should be small.

The design of SMC involves two tasks. The first one is to select the switching hyperplane $s(x, t)$ to prescribe the desired dynamic characteristics of the controlled system. The second one is to design the discontinuous control such that the system enters the sliding mode $s(x, t) = 0$ and remains in it forever [3, 14].

In this paper, we use the sliding surface proposed par J.J. Slotine,

$$s(x, t) = \left(\frac{d}{dt} + \lambda \right)^{n-1} e(t) \quad (10)$$

in which $e = x_d(t) - x(t)$, λ is a positive coefficient, and n is the system order.

It remains to be shown that the control law can be constructed so that the sliding surface will be reached. Then, a sliding hyperplane S can be represented as $s(x, t) = 0$.

The scalar $s(x, t)$ is defined as the distance to the sliding hyperplane S .

Consider a Lyapunov function:

$$V = \frac{1}{2} s^2 \quad (11)$$

From Lyapunov theorem we know that if \dot{V} is negative definite, the system trajectory will be driven and attracted toward the sliding surface and remain sliding on it until the origin is reached asymptotically [6]:

$$\dot{V} = s \dot{s} \quad (12)$$

The simplified 1st order problem of keeping the scalar $s(x,t)$ at zero can be achieved by choosing the control law $u(t)$. A sufficient condition for the stability of the system is

$$\frac{1}{2} \frac{\partial}{\partial t} s^2 \leq -\eta |s| \quad (13)$$

where η is a positive constant. (13) is called reaching condition or sliding condition.

If the control input is so designed that the inequality (13) is satisfied, together with the properly chosen sliding hyperplane, the state will be driven toward the origin of the state space along the sliding hyperplane from any given initial state. This is the way of the SMC that guarantees asymptotic stability of the systems.

The process of sliding mode control can be divided in two phases, that is, the approaching phase and the sliding phase. The sliding mode control law $u(t)$ consists of two terms, equivalent term $u_{eq}(t)$, and switching term $u_s(t)$.

In the sliding phase, where $s(x,t)=0$ and $\dot{s}(x,t)=0$, the equivalent term $u_{eq}(t)$ is designed to keep the system on the sliding surface. In the approaching phase, where $s(x,t) \neq 0$, the switching term $u_s(t)$ is designed to satisfy the reaching condition (13).

While in sliding phase we have:

$$\dot{s}(x,t) = 0 \quad (14)$$

By solving the above equation formally for the control input, we obtain an expression for u called the equivalent control u_{eq} .

In order to satisfy sliding conditions (13) and to despite uncertainties on the dynamic of the system, we add a discontinuous term across the surface $s(x,t)=0$, so the sliding mode control law $u(t)$ has the following form:

$$\begin{aligned} u &= u_{eq} + u_s \\ u_s &= -K_f \operatorname{sgn}(s(x,t)) \end{aligned} \quad (15)$$

where K_f is the control gain.

For a defined function φ :

$$\operatorname{sgn}(\varphi) = \begin{cases} 1, & \text{if } \varphi > 0 \\ 0, & \text{if } \varphi = 0 \\ -1, & \text{if } \varphi < 0 \end{cases} \quad (16)$$

The controller described by the equation (14) presents high robustness, insensitive to parameter fluctuations and disturbances [1, 3, 4, 15, 16], but it will have high-frequency

switching (chattering phenomena) near the sliding surface due to sgn function involved. These drastic changes of input can be avoided by introducing a boundary layer with width ε [3, 4, 16, 17]. Thus replacing $\text{sgn}(s(t))$ by $\text{sat}(s(t)/\varepsilon)$ in (15), we have

$$u = u_{eq} - K_f \text{sat}(s(x,t)/\varepsilon) \quad (17)$$

Where

$$\varepsilon > 0,$$

$$\text{sat}(\varphi) = \begin{cases} \text{sgn}(\varphi) & \text{if } |\varphi| \geq 1 \\ \varphi & \text{if } |\varphi| < 1 \end{cases}.$$

3.1 Position Control

The position error is defined by:

$$e = \theta_{ref} - \theta \quad (18)$$

For $n=2$, the position control manifold equation can be obtained from equation (10) as follows:

$$s(e) = \lambda_\theta e + \frac{d}{dt} e \quad (19)$$

The equation of the motion (2) can be rewritten:

$$\ddot{\theta} = -\frac{B}{J}\dot{\theta} + \frac{p\lambda}{J}i_{qs} - \frac{p}{J}T_r \quad (20)$$

$$s(\theta) = \lambda_\theta \dot{\theta} - \lambda_\theta \dot{\theta}_{ref} + \ddot{\theta}_{ref} - \ddot{\theta} \quad (21)$$

$$\dot{s}(\theta) = \lambda_\theta \dot{\theta}_{ref} + \ddot{\theta}_{ref} + \left(\frac{B}{J} - \lambda_\theta\right)\dot{\theta} + \frac{pT_r}{J} - \frac{p\lambda}{J}i_{qs} \quad (22)$$

During the sliding mode and in permanent regime, we have

$$s(\theta) = 0, \dot{s}(\theta) = 0, i_{sq}^n = 0$$

The current control i_{qs} is defined by:

$$i_{qs} = i_{qs}^{eq} + i_{qs}^n \quad (23)$$

In which:

$$i_{qs}^{eq} = \frac{J}{p\lambda} \left(\lambda_{\theta} \dot{\theta}_{ref} + \ddot{\theta}_{ref} + \left(\frac{B}{J} - \lambda_{\theta} \right) \dot{\theta} + \frac{pT_r}{J} \right) \quad (24)$$

$$i_{qs}^n = K_{\omega} \operatorname{sgn}(s(\Omega)) \quad (25)$$

K_{ω} – positive constant.

3.2. Direct Current Controller

The direct current error is defined by:

$$e_d = i_{dref} - i_{ds} \quad (26)$$

For $n=1$, the direct current control manifold equation can be obtained from equation (10) as follows:

$$s(i_{ds}) = i_{dref} - i_{ds} \quad (27)$$

$$\dot{s}(i_{ds}) = \dot{i}_{dref} - \dot{i}_{ds} \quad (28)$$

Substituting the expression of i_{ds} given by equation (1) and (4) in equation (28) we obtain:

$$\dot{s}(i_{ds}) = \frac{d}{dt} i_{dref} + \frac{R_s}{L_{ds}} i_{ds} - \frac{L_{qs}}{L_{ds}} i_{qs} \omega - \frac{1}{L_{ds}} v_{ds} \quad (29)$$

During the sliding mode and in permanent regime, we have

$$s(i_{ds}) = 0, \dot{s}(i_{ds}) = 0, v_{ds}^n = 0$$

The control voltage v_{dref} is defined by:

$$v_{dref} = v_{ds}^{eq} + v_{ds}^n \quad (30)$$

Where:

$$v_{ds}^{eq} = \left(\frac{d}{dt} i_{dref} + \frac{R_s}{L_{ds}} i_{ds} - \frac{L_{qs}}{L_{ds}} i_{qs} \omega \right) L_{ds} \quad (31)$$

$$v_{ds}^n = K_d \operatorname{sgn}(s(i_d)) \quad (32)$$

K_d – positive constant.

3.3. Quadrature Current Control

The quadrature current error is defined by:

$$e_q = i_{qref} - i_{qs} \quad (33)$$

For $n=1$, the quadrature current control manifold equation can be obtained from equation (10) as follows:

$$s(i_{qs}) = i_{qref} - i_{qs} \quad (34)$$

Then, we have

$$\dot{s}(i_{qs}) = \dot{i}_{qref} - \dot{i}_{qs} \quad (35)$$

Substituting the expression of \dot{i}_{qs} given by equation (1) and (8) in equation (35) we obtain:

$$\dot{s}(i_{qs}) = \frac{d}{dt} i_{qref} + \frac{R_s}{L_{qs}} i_{qs} + \frac{L_{ds}}{L_{qs}} \omega i_{ds} + \frac{M_{fd}}{L_{qs}} \omega i_f + \frac{1}{L_{qs}} v_{qs} \quad (36)$$

During the sliding mode and in permanent regime, we have

$$s(i_{qs}) = 0, \dot{s}(i_{qs}) = 0, v_{qs}^n = 0$$

The control voltage v_{qref} is defined by:

$$v_{qref} = v_{qs}^{eq} + v_{qs}^n \quad (37)$$

Where:

$$v_{qs}^{eq} = \left(\frac{d}{dt} i_{qref} + \frac{R_s}{L_{qs}} i_{qs} + \frac{L_{ds}}{L_{qs}} \omega i_{ds} + \frac{M_{fd}}{L_{qs}} \omega i_f \right) L_{qs} \quad (38)$$

$$v_{qs}^n = K_q \operatorname{sgn}(s(i_{qs})) \quad (39)$$

K_q – positive constant.

4 LOAD TORQUE OBSERVER

The motion equation of synchronous machine (2) can be expressed in state space as follows:

$$\begin{aligned} \dot{X} &= \mathbf{A} X + \mathbf{B} u \\ Y &= \mathbf{C} X \end{aligned} \quad (40)$$

$$\text{Where } X = \begin{bmatrix} \Omega \\ T_L \end{bmatrix}, u = i_{qs}, \mathbf{A} = \begin{bmatrix} -\frac{B}{J} & -\frac{1}{J} \\ 0 & 0 \end{bmatrix}, \mathbf{B} = \begin{bmatrix} \lambda \\ 0 \end{bmatrix}, \mathbf{C} = \begin{bmatrix} 1 \\ 0 \end{bmatrix}.$$

It is well known that observer is available when input is unknown and inaccessible. For simplicity a 0-observer is selected. In this paper, the load torque T_L is estimated by using an observer. A linear asymptotic observer is designed in the same form as the original system

(40) with an additional input depending on the mismatch between the real values and the estimated values of the output vector [17, 18]. The system equation can be expressed as:

$$\dot{\hat{X}} = \mathbf{A}\hat{X} + \mathbf{B}u + \mathbf{L}(Y - \mathbf{C}\hat{X}) \quad (41)$$

Where $\mathbf{L} = \begin{bmatrix} L_1 \\ L_2 \end{bmatrix}$

Where \hat{X} is an estimate of the system state vector, and L is the proportional gain vector to be chosen so as to achieve prespecified error characteristics.

The motion equation with respect to mismatch $\tilde{X} = \hat{X} - X$ is of form

$$\dot{\tilde{X}} = (\mathbf{A} - \mathbf{LC})\tilde{X} \quad (42)$$

The behavior of the mismatch governed by homogeneous equation is determined by the eigenvalues of the matrix $(\mathbf{A} - \mathbf{LC})$. For the observable system they may be assigned arbitrarily by a proper choice of the gain vector L . It means that any desired rate of convergence of the mismatch to zero or estimate $\hat{X}(t)$ to the state vector $X(t)$ may be provided. To ensure that the observer is stable the instantaneous eigenvalues of the observer have to be placed in the left half side plane. The characteristics equation is given by:

$$\text{Det} [p\mathbf{I} - (\mathbf{A} - \mathbf{LC})] = 0 \quad (43)$$

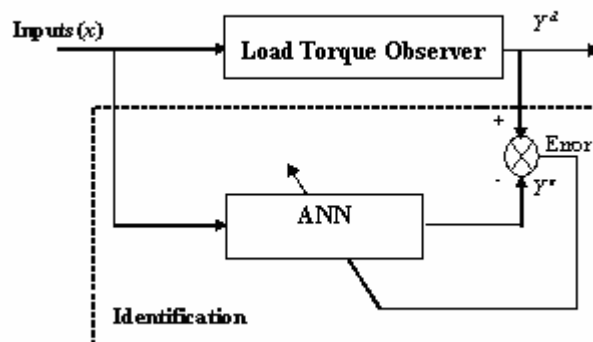
Where \mathbf{I} is the identity vector, and p is the Laplace operator.

The gain vector L is defined by imposing the poles in the characteristics equation.

5 DESIGN OF A NEURAL NETWORK LOAD TORQUE OBSERVER

Artificial Neural Networks (ANN's) are potential candidates for approximating complex non-linear process dynamics and have been used to formulate a variety of control strategies.

In this section, a Multi Layer Perceptron (MLP) neural network is applied to load torque observer identification. The neural network observer is trained to approximate the load torque observer described in section 4.



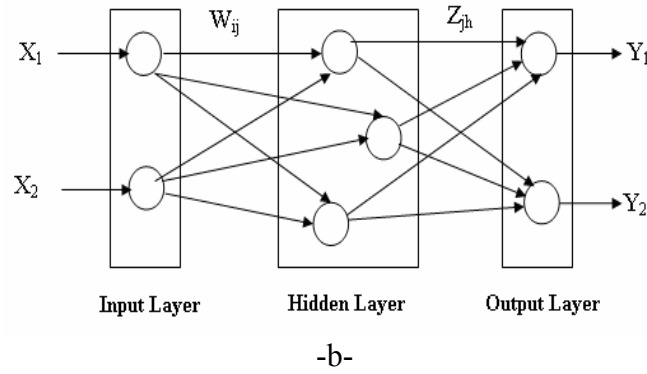


Fig. 3. Supervised training of artificial neural networks: a) identification of the load torque observer; b) structure of ANN

Figure (3-b) shows the structure of a feedforward multi-layer network with two input and two output signals. The topology is based on Perceptron which was proposed by Rosenblatt in 1958.

The network has three layers, defined as input layer, hidden layer, and output layer. The nodes represent neurons and the dots in the connections represent the weights. The summing nodes accumulate all the input weighted signals and then pass to the output through the transfer function [19]. The transfer function most commonly used is the sigmoidal transfer function, and it is given by

$$Y = \frac{1}{1 + e^{-\alpha x}} \quad (44)$$

where α is the coefficient or gain which adjusts the slope of the function. With high gain, this function approaches a step function.

Back-Propagation training algorithm is most commonly used in a feedforward neural networks as mentioned before. Figure (4) shows the principle of back-propagation training.

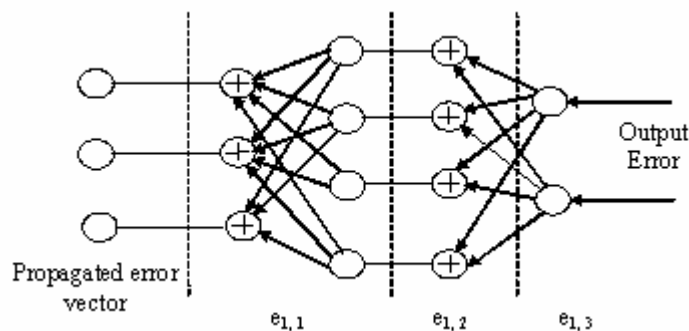


Fig. 4. Principle of Back-Propagation training.

In the beginning, the network is assigned random positive and negative weights. For a given input signal pattern, step by step calculations are made in the forward direction to derive the output pattern. A cost functional given by the squared difference between the net output and the desired net output for the set of input patterns is generated and this is minimized by gradient descent method altering the weights one at time starting from the

output layer. For the input pattern p , the squared output error for all the output layer neurons of the network is given as

$$E_p = \frac{1}{2}(d^p - y^p)^2 = \frac{1}{2} \sum_{j=1}^S (d_j^p - y_j^p)^2 \quad (45)$$

Where d_j^p is the desired output of the j^{th} neuron in the output layer, y_j^p is the corresponding actual output, S is the dimension of the output vector, y^p is the actual net output vector, and d^p is the corresponding desired output vector. The total squared error E for the set of P patterns is then given by

$$E = \frac{1}{2} \sum_{p=1}^P E_p = \frac{1}{2} \sum_{p=1}^P \sum_{j=1}^S (d_j^p - y_j^p)^2 \quad (46)$$

The weights are changed to reduce the cost functional E in a minimum value by gradient descent method, as mentioned. The weight update equation is then given as

$$W_{ij}(t+1) = W_{ij}(t) + \eta \left(\frac{\delta E_p}{\delta W_{ij}(t)} \right) \quad (47)$$

Where η is the learning rate, $W_{ij}(t+1)$ is the new weight and $W_{ij}(t)$ is the old weight. The weights are updated for all the P training patterns. Sufficient learning is achieved when the total error E summed over the patterns falls below a prescribed threshold value. The iterative process propagates the error back-propagation [19, 20, 21].

6 SIMULATION AND RESULTS

In this section, we simulate the system described in figure (1). The position and currents loops of the drive were also designed and simulated respectively with sliding mode control. The feedback control algorithms were iterated until best simulation results were obtained.

The position loop was closed, and transient response was tested with both current controller and position control. The simulation of the starting mode without load is done, followed by reversing of the reference $\theta_{ref} = \pm 3 \text{ rad/s}$ at $t_3=2\text{s}$.

The load (T_L) is applied in two period:

1. The reference $\theta_{ref} = +3 \text{ rad}$, the load ($T_L = +8\text{Nm}$) is applied at $t_1 = 1 \text{ s}$ and eliminated at $t_2 = 1.5 \text{ s}$
2. The reference $\theta_{ref} = -3\text{rad}$, the load ($T_L = -8\text{Nm}$) is applied at $t_4 = 3 \text{ s}$ and eliminated at $t_5 = 3.5 \text{ s}$.

The simulation is realized using the SIMULINK software in MATLAB environment.

Figure (5) shows the performances of the sliding mode controller.

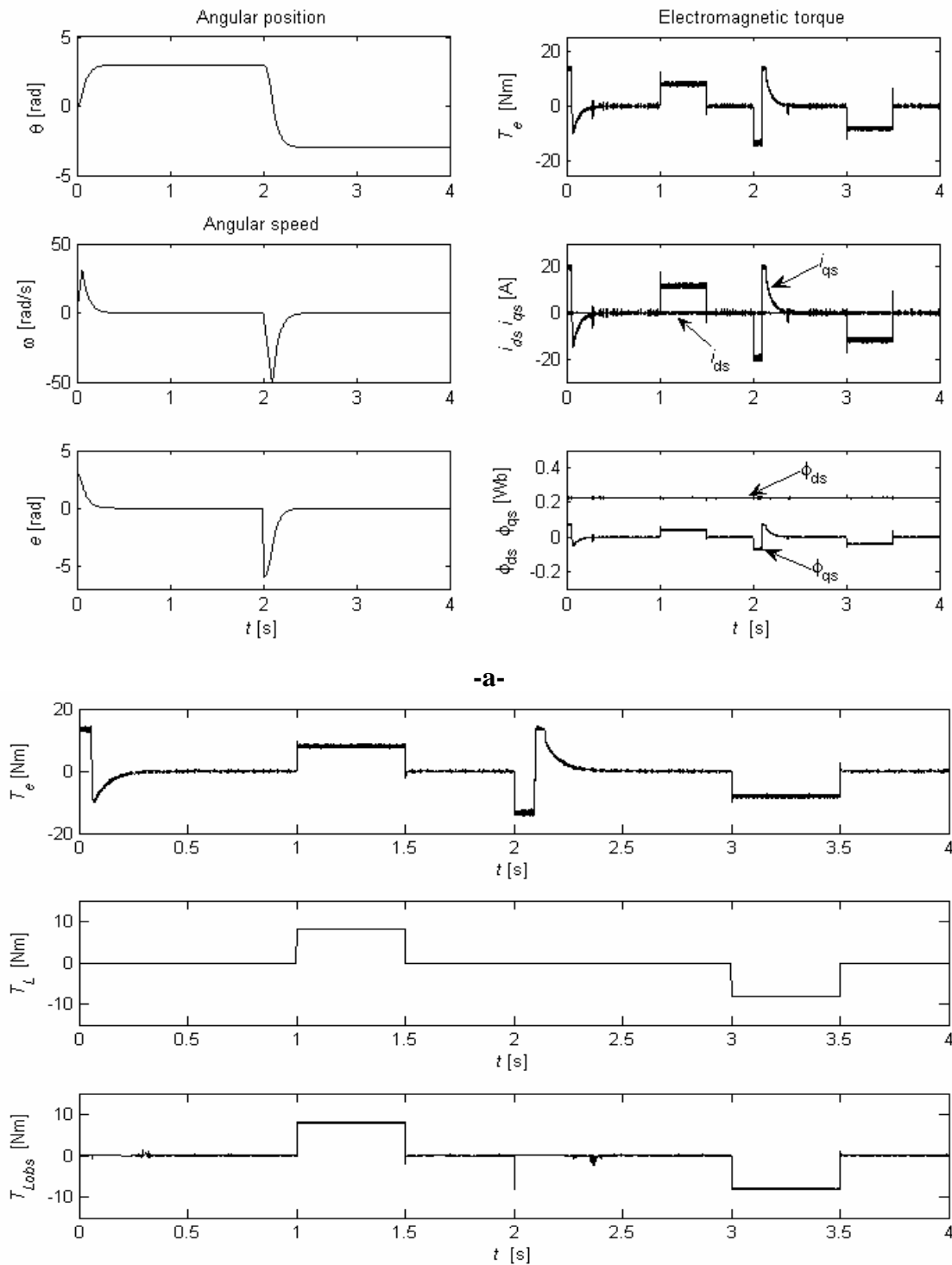


Fig. 5. Simulation results of position controller: a- Response of the system; b- Response of the Neural load torque observer (input: 2, hidden layer: 4-10, output: 1) .

The control presents the best performances, to achieve tracking of the desired trajectory. The sliding mode controller rejects the load disturbance rapidly with no overshoot and with a negligible steady state error. The current is limited in its maximal admissible value by a saturation function. The decoupling of torque-flux is maintained in permanent regime. The neural load torque observer is used successfully without affecting the system response.

Robustness

In order to test the robustness of the used method we have studied the effect of the parameters uncertainties on the performances of the position control. We have simulated the system with different values of the parameter considered and compared to nominal value (real value).

Two cases are considered:

1. The moment of inertia ($\pm 50\%$).
2. The stator and rotor resistances ($+80\%$).

To illustrate the performances of control, we have simulated the starting mode of the motor without load, and the application of the load ($T_L = +8\text{Nm}$) at the instance $t_1 = 1\text{ s}$ and it's elimination at $t_2 = 2\text{ s}$; in presence of the variation of parameters considered (the moment of inertia, the stator resistances) with position step of $+3\text{ rad/s}$.

Figure (6) shows the tests of robustness realized with the sliding mode control for different values of the moment of inertia.

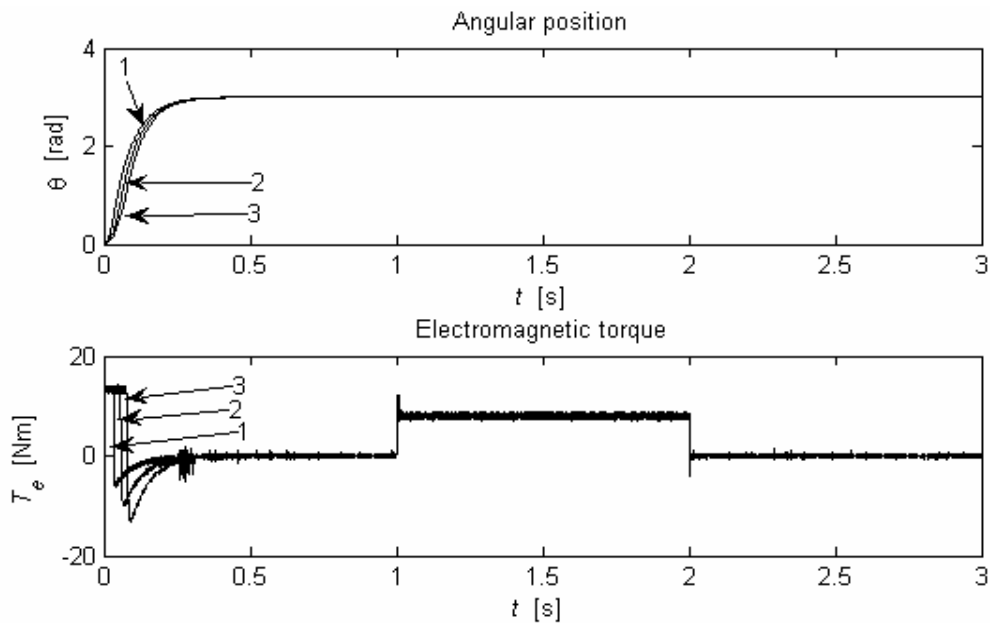


Fig. 6. Test of robustness for different values of the moment of inertia: 1) – 50%, 2) nominal case, 3) +50%.

Figure (7) shows the tests of robustness realized with the sliding mode control for different values of stator and rotor resistances.

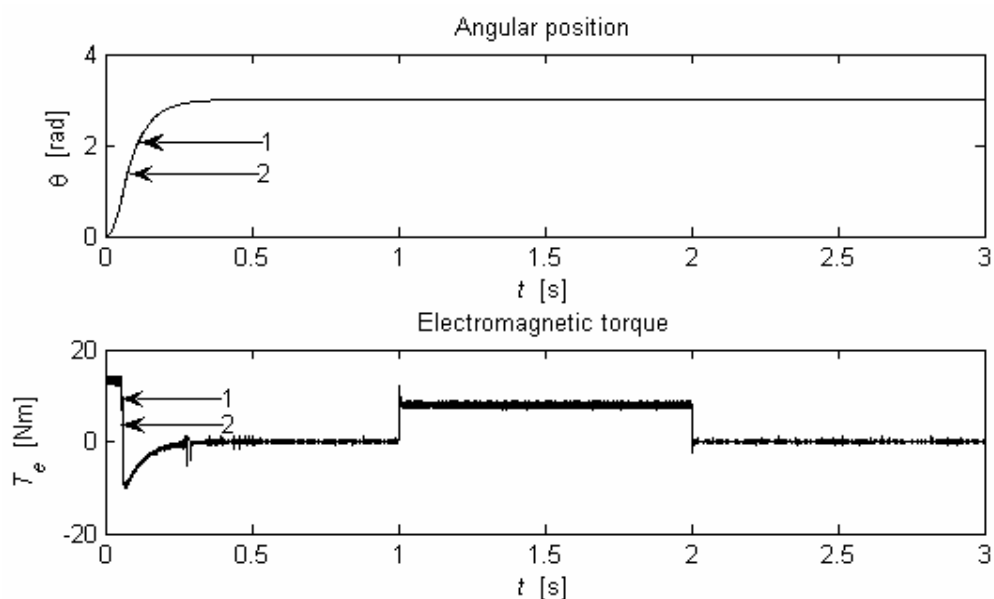


Fig. 7. Test of robustness for different values of stator and rotor resistances: 1) nominal case, 2) +80%.

For the robustness of control, a decrease or increase of the moment of inertia J , the stator resistances doesn't have any effects on the performances of the technique used (Figures 6 and 7). An increase of the moment of inertia gives best performances, but it presents a slow dynamic response (Figure 6). The sliding mode control gives to our controller a great place towards the control of the system with unknown parameters.

7 CONCLUSION

In this study, a numerical simulation of the vector control of the self controlled synchronous motor is done using a sliding mode control. The paper develops a simple robust controller to deal with parameters uncertain and external disturbances and takes full account of system noise, digital implementation and integral control.

A neural load torque observer is developed and used successfully. The global system with load torque observer was analyzed and designed, and performances were studied extensively by simulation to validate the theoretical concept. The simulation study clearly indicates the superior performance of the sliding mode control, because it is inherently adaptive in nature. It appears from the response properties that it has a high performance in presence of the plant parameters uncertain and load disturbances. The control of position by SMC gives fast dynamic response with no overshoot and negligible steady-state error. With good choice of control parameters, the chattering phenomena is minimized, the torque fluctuations are reduced, the limitation of the current is ensured by a saturation function.

APPENDIX

Three phases SM parameters:

Rated output power 3HP, Rated phase voltage 60V, Rated phase current 14 A, Rated field voltage $v_f=1.5V$, Rated field current $i_f=30A$, Stator resistance $R_s=0.325\Omega$, Field resistance $R_f=0.05\Omega$, Direct stator inductance $L_{ds}=8.4$ mH, Quadrature stator inductance $L_{qs}=3.5$ mH,

Field leakage inductance $L_f=8.1\text{mH}$, Mutual inductance between inductor and armature $M_{fd}=7.56\text{mH}$, The damping coefficient $B=0.005\text{ N.m/s}$, The moment of inertia $J=0.05\text{ kg.m}^2$, Pair number of poles $p=2$.

REFERENCES

- [1] Utkin V. I.: Variable structure system with sliding modes. IEEE Trans. on Automatic Control, vol. AC-22, April 1977, 210–222.
- [2] David Young K., V. I. Utkin and Ümit Özgüner: A control engineer's guide to sliding mode control. IEEE Trans. on Control Systems Technology, Vol. 7, No. 3, May 1999.
- [3] Slotine J. J. E., W. Li: Applied nonlinear control. Prentice Hall, USA, 1998.
- [4] Astrom K. J. , B. Wittenmark: Adaptive control. Addison-Wesley, 1989.
- [5] Guldner J., V. I. Utkin. The chattering problem in sliding mode systems. Fourteenth International Symposium of Mathematical Theory of Networks and systems, MTNS2000, June 19-23, 2000, Perpignan, France.
- [6] Buhler H. : Réglage par mode de glissement. Presses polytechniques romandes, Lausanne, 1986.
- [7] Utkin V.I.: Sliding mode control design principles and applications to electrical drives. IEEE Trans. on Industrial Electronics, vol. 40, NO. 1, February 1993, 23-36.
- [8] Utkin V. I. , A. Šabanović. Sliding modes applications in power electronics and motion control systems. IEEE, International Symposium on Industrial Electronics, Vol. 1, July 1999, pp 22-31.
- [9] Bose B. K.. Power electronics and AC drives. Prentice Hall, Englewood Cliffs, Newjersey, 1986.
- [10] Guy Sturtzer, Eddie Smigiel. Modélisation et commande des moteurs triphasés. edition Ellipses, 2000.
- [11] Kendouci K.: Etude comparative des différentes commandes de la machine synchrone à aimants permanents. Thèse de Magister, Université de science technologique d'Oran, septembre 2003.
- [12] Cambronne J.P., Le Moigne Ph., et Hautier J.P.: Synthèse de la commande d'un onduleur de tension. J. Phys III France pp757-778, 1996.
- [13] Ji Chang Lo, Ya Hui Kuo: Decoupled fuzzy sliding mode control. IEEE Trans. on Fuzzy Systems, vol. 6, N°3, August 1998.
- [14] Abid M., Y. Ramdani, A. Bendaoud, A. Meroufel. Réglage par mode glissant d'une machine asynchrone sans capteur mécanique. Rev. Roum. Sci. Techn. – Electrotechn. et Energ., 2004, 406–416.
- [15] Utkin V. I.: Sliding modes and their application in variable structure system. MIR, Moscow, 1978.
- [16] Khalil, H. K. : Non linear system. MacMillan, New York, 1992.
- [17] Ko, J. S. , J. H. Lee, S. K. Chung, and M.J. Youn: A robust position control of Brushless DC motor with Dead Beat Load Torque observer, IEEE Transaction on industrial Electronics, vol. 40, no. 5, pp. 512-520, 1999.
- [18] Grellet G., G. Clerc: Actionneur électrique : principe, modèle, commande, Edition EYROLLES, 1997.
- [19] Bose B. K.: "Expert System, Fuzzy logic, and neural network Applications in power Electronics and motion control", *Proceedings of the IEEE*, Vol. 82, NO. 8 August 1994, 1303-1321.

-
- [20] Baghli L.: Contribution à la commande de la machine asynchrone, utilisation de la logique floue, des réseaux de neurone et des algorithmes génétiques. Thèse de doctorat, S.T.I.M.A- NANCY, 1999.
- [21] M. Chow, R. N. Sharpe and J. C. Hung, "On the application and design of artificial neural networks for motor fault detection – Part I", *IEEE Transaction on Industry Electronics*, Vol. 40, NO. 2 April 1993, 181-188.